ISSN 1996-5044

Research Journal of

Nanoscience and Nanotechnology

http://knowledgiascientific.com

Knowledgia SCIENTIFIC
A Place to Publish Outstanding Research

OPEN ACCESS Research Journal of Nanoscience and Nanotechnology

ISSN 1996-5044
DOI: 10.3923/rjnn.2020.15.26

Review Article
Sonochemical Method Preparation of Nanosized Systems Based on Oxides of Zn, Ce and Mo

[1]Valery Zazhigalov, [1]Olena Sachuk and [2]Volodymyr Starchevskyy

[1]Institute for Sorption and Problems of Endoecology , Ukraine National Academy of Science, Ukraine
[2]Lviv Polytechnic National University, Lviv, Ukraine

Abstract

The influence of sonochemical treatment on the physico-chemical properties of oxide systems ZnO/CeO_2, ZnO/MoO_3 and CeO_2/MoO_3 were investigated and changes in crystalline structure, morphology and phase transformation was established. It was found that as a result of the treatment the formation of triclinic modification of zinc molybdate α-$ZnMoO_4$, grinding of the oxides and increase of specific surface area of the compositions occurs. The results of catalytic activity of activated samples in ethanol oxidation reaction demonstrate the high selectivity and yield of acetic aldehyde (94%) at low reaction temperature. The blue shift of edge absorption in powder-like samples and band-gap energy (Eg) increase were fixed by UV-vis spectroscopy. It was found that activated samples show the promising results in dyes photodegradation processes of water solution at visible light irradiation.

Key words: Sonochemical treatment, oxide composition, zinc molybdate, cerium oxide, molybdena, ethanol, acetic aldehyde

Citation: Valery Zazhigalov, Olena Sachuk and Volodymyr Starchevskyy, 2020. Sonochemical method preparation of nanosized systems based on oxides of Zn, Ce and Mo. Res. J. Nanosci. Nanotechnol., 10: 15-26.

Corresponding Author: Valery Zazhigalov, Institute for Sorption and Problems of Endoecology, Ukraine National Academy of Science, Ukraine

Competing Interest: The authors have declared that no competing interest exists.

Data Availability: All relevant data are within the paper and its supporting information files.

INTRODUCTION

The development of modern technologies based on the effect of ultrasound radically differs from the traditional methods synthesis of new materials which require the use of metal salts, solvents and heating etc. Sonochemical treatment permits to exclude some limitations of these technological processes and opens the possibility of creating on their basis non-waste, environmentally friendly and low-cost methods of production materials[1]. Herewith, the chemical processes intensification, the change of physical and chemical properties and the preparation of heterogeneous systems in a nanodispersed state is an integrant ability of this method[2,3]. The effect of ultrasound on liquid-phase systems is based on the phenomenon of acoustic cavitation, which occurs in a liquid as a result of a local decrease in pressure during the passage of an acoustic wave of high intensity[4]. Herewith as a result of treatment the bubbles filled with gas, fluid pairs are formed, which are flushed in the next stage of the increase of pressure. This process accompanied by the solids particles destruction and as result of new surface appearance the molecules adsorption and formation of solvation shells can proceed. The formation of uncompensated physical and chemical bonds on the solid surface makes easier the interaction between molecules with formation of new chemical compounds. The investigations of sonochemical reactions and kinetic of this process in more detail were described earlier[1,3-8].

It should be noted that lately much attention is paid to the ultrasonic synthesis of some metal oxides[9-27] among of which the leading place belongs to oxides of molybdenum, zinc and cerium as perspective catalysts, semiconductors, powder lasers, electrochemical pumps and luminescent materials etc. Jeevanandam *et al.*[15], Chen *et al.*[16], Bin *et al.*[17], Krishnan *et al.*[18], Manivel *et al.*[19], Pholnak *et al.*[20], Costa *et al.*[21], Arruda *et al.*[22], Kandjani *et al.*[23], Tabatabee *et al.*[24], Zhang *et al.*[25], Wang *et al.*[26] and Wang *et al.*[27] reported the possibility of sonochemical synthesis of stable nanodispersed particles of MoO_3, ZnO and CeO_2 under different conditions of the process such as; Media nature, time processing and solution concentration were shown. Presented data in these publications showed the change of morphology, crystalline structure, catalytic and optical properties under the ultrasonic action, but simultaneously demonstrated the absence of the data of its effect on the properties of two-component systems.

This study was aimed to analyze experimental researches of Ultrasonic Treatment (UST) of ZnO/MoO_3, CeO_2/MoO_3 and ZnO/CeO_2 systems with molar ratio of initial components of the mixture 1:1 on their physico-chemical properties.

ULTRASONIC TREATMENT OF BINARY SYSTEMS BASED ON MoO_3, ZnO AND CeO_2

Sonoactivation of ZnO/MoO_3 system: The results of the sonochemical treatment of ZnO and MoO_3 mixtures with different molar ratio of oxides were reported in previous publication[28]. It was found that ultrasonic activation of the mixture with equimolar ratio of initial oxides (ZnO/MoO_3 = 1:1) permits to obtain nanosized $ZnMoO_4$ triclinic modification[28,29]. Activation of oxides mixture was conducted to use the magnetostrictive emitter as the source of ultrasound, herewith the waveguide was immersed in the test mixture and connected to the UZDN-2T ultrasonic generator. The aqueous solutions of the samples were treated during 1 h at frequency of 22-40 kHz the temperature of reaction medium was 80°C. The obtained emulsions were dried in air at 110°C. The rest of the samples (CeO_2/MoO_3 and ZnO/CeO_2 systems) were treated similarly.

Figure 1 presents the XRD patterns of ZnO/MoO_3 = 1:1 composition. In contrast to initial sample where peaks of α-MoO_3 orthorhombic modification with dominant intensity reflex from the plane [040] and diffraction peaks of ZnO with wurtzite hexagonal structure present on the diffractogram of this composition UST leads to significant changes in the view of XRD patterns as presented in Fig. 1a. Firstly, a decrease of reflexes intensity of initial oxides that can be due to dimension of their crystallites size is occurred (Table 1). Secondly, after ultrasonic modification in XRD of the sample an appearance of new reflexes which are belong to zinc molybdate phase α-$ZnMoO_4$ triclinic modification was observed. The maximal intensity observed for reflex from the plane [114] (Fig. 1b). In ultrasonic process the solid phase reaction between initial components of ZnO and MoO_3 with formation of new compound α-$ZnMoO_4$ takes place.

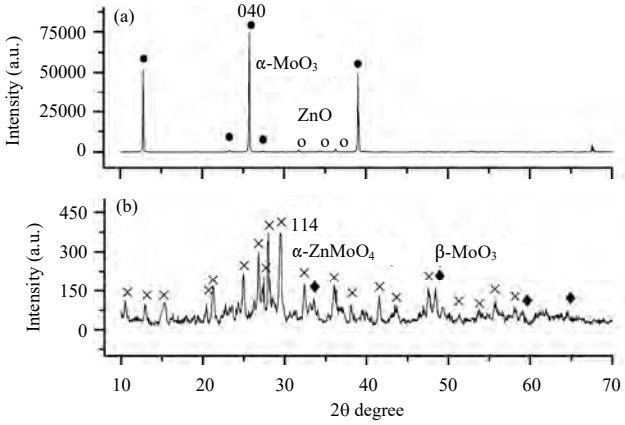

Fig. 1(a-b): Diffractograms of a initial sample, (a) Zn/Mo = 1:1 and (b) After its 1 h UST
UST: Ultrasonic treatment

Table 1: Some properties of ZnO/MoO_3 = 1:1 composition

				Catalytic properties at X = 100%		
Samples	*L (nm)	S_{BET} ($m^2 g^{-1}$)	V_Σ ($cm^3 g^{-1}$)	T_r (°C)	S (CH_3CHO)	S(C_2H_4)
Initial	81	2	0.03	317	81	19
After UST	33	6	0.06	255	94	6

L: Average crystallite size, determined from the maximum intensive reflex, S_{BET}: Specific surface area (BET) of the sample, V_Σ: Total pore volume, T_r: Reaction temperature, S: Selectivity of the product and X: Ethanol conversion

Table 2: Results of EDS analysis of the samples ZnO/MoO_3 = 1:1 composition

		Element content (%)	
Samples	Analysis site	Zn	Mo
Initial	A	4.4	95.6
	B	97.0	3.0
	Full surface	49.2	50.8
After UST	A	49.9	50.1
	B	48.4	51.6
	Full surface	48.9	51.1

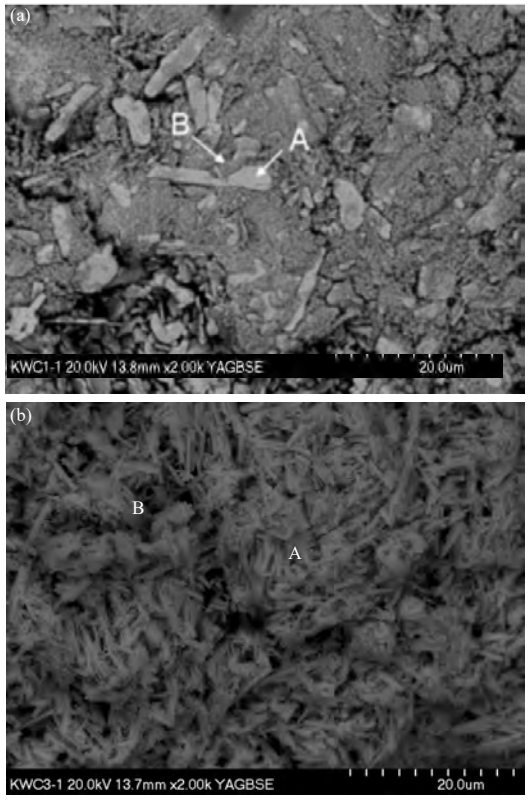

Fig. 2(a-b): SEM images of ZnO/MoO_3 = 1:1 composition, (a) Initial and (b) After UST
UST: Ultrasonic treatment

Traditionally this phase was prepared from salts of these metals in the different organic mediums and by annealing[30-32] about 1000°C.

Simultaneously on the diffractogram there are the reflexes of weak intensity which can be attributed by monoclinic modification of molybdena β-MoO_3. The formation of this phase can be connected with anisotropic destruction of α-MoO_3. It was hypothesized that the formation of this molybdena modification can accelerate the zinc molybdate formation or be initial compound in this process, but the possibility of the formation of zinc molybdate due to reaction between hydrated molybdenum and zinc oxides as suggested in Keereeta *et al.*[30], Ait ahsaine *et al.*[31], Agarwal *et al.*[32], Karekar *et al.*[33] and Zhang *et al.*[34] is not excluded.

The study of the samples properties by low-temperature nitrogen adsorption method showed some changes of their structure after sonochemical activation. Some parameters of porous structure of the samples are presented in Table 1. It can be seen that initial mixture ZnO/MoO_3 = 1:1 characterized by low adsorption parameters, however after its treatment the increase of specific surface area and total pore volume was observed. Similar changes in ZnO/MoO_3 system were fixed after its mechanochemical treatment[35-37]. In this case, such changes can be connected with dispersion of the sample which was established by XRD method. From the other hand, it was found that ultrasonic as well mechanochemical treatment of the compounds with low specific surface area (i.e., non-porous) leads to formation of a secondary porous structure. The increase of porous structure parameters was observed after 2 h of UST as reported by Zazhigalov *et al.*[29].

The morphology of ZnO/MoO_3 samples was observed by SEM (Fig. 2a, b) and TEM (Fig. 3a, b) methods. From the SEM images of initial ZnO/MoO_3 = 1:1 composition (Fig. 2a) (as well from the TEM data (Fig. 3a)), the two types particles with different morphology were observed. Namely big oblong crystals (a) which according to EDS analysis belong to molybdenum oxide and small irregular crystals (b) which correspond to zinc oxide present in initial sample. The conducted researches show a high degree homogenization of the sample after treatment. As presented in Fig. 2b sonoactivation leads to formation of significant number of elongate crystals, which can characterized the appearance of zinc molybdate. Similar structure of formed α-$ZnMoO_4$ was observed in previous studies[30,34].

The data presented in Table 2 showed that the ratio of Zn/Mo in elongate crystals independently from analysis places (A, B, full surface) is about one which is in agreement with XRD data permits to attribute them to α-$ZnMoO_4$.

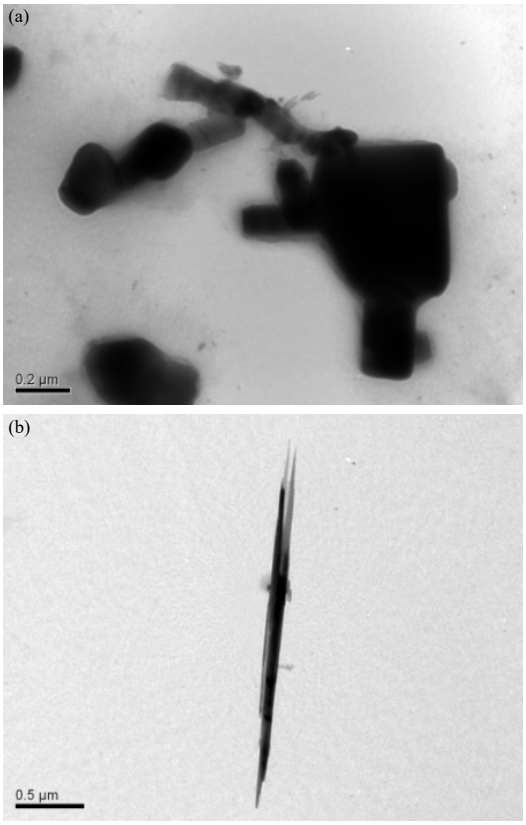

Fig. 3(a-b): TEM images of ZnO/MoO_3 = 1:1 composition, (a) Initial and (b) After its UST

Table 3: FT-IR data of ZnO/MoO3 = 1:1 composition

Absorption band samples	Wave number (cm^{-1})				
	Mo=O	Mo-O-Mo	Zn-O	O-Mo-O	Mo-O-Zn
Initial	988	860	500	-	-
After UST	924	897	500	655	531

Results obtained by TEM methods are in good agreement with SEM and XRD data. Figure 3b showed that the sample after treatment displayed the presence of needle-like shapes crystals with an average dimension of cross section 70-130 nm and length of 0.5-5 µm.

So, the study of the samples ZnO/MoO_3 = 1:1 composition after its sonochemical treatment show that in UST process not only the decrease of the oxides particle size, but chemical reaction between oxides with formation of α-$ZnMoO_4$ in form of needle-like crystals were occurred.

The changes of sample morphology and the decrease of crystallite sizes resulting from UST process are accompanied by a change in the IR spectra (Table 3). The IR spectrum of initial mixture ZnO/MoO_3 shows the presence of absorption bands at 988, 860 and 500 cm^{-1}, which correspond to the stretching modes of the Mo=O terminal bond, Mo_2O (Mo-O-Mo) entity[38,39] and stretching vibrations of Zn-O bond[40,41], respectively.

As a result of sonochemical treatment some changes in spectrum of the sample are observed. These changes are connected with a shifting of absorption bands of stretching vibrations of terminal Mo=O and linear Mo-O-Mo bonds in α-MoO_3 and an appearance of new bands at 655 and 531 cm^{-1}. Last vibrations can be determined as O-Mo-O and Mo-O-Zn bonds, respectively. Their appearance can be connected with formation of zinc molybdate phase[42] that was observed by XRD. So, the data of IR spectroscopy have good agreement with results of these samples study by XRD, SEM and TEM methods.

According to DTA-TG, the treatment accompanied by the some changes on the obtained thermograms. Studied samples were heated from ambient to 800°C under air flow and heating rate was 10°C min^{-1}, sample weight was equal to 200 mg. Thermogram of initial sample is characterized by the presence of two endothermal effects: (1) First was observed at 140-208°C on the DTA curve which is accompanied by weight loss (about 6%) and primarily due to the loss of non-dissociative adsorbed water as well as water connected with the surface by hydrogen bond and (2) Second (without mass loss) was observed at 792°C which corresponds to melting of α-MoO_3. In the case of sonotreated sample the process of its surface dehydroxylation characterized by the presence of two minor endothermal effects in temperatures region of 75-300°C (maximum were observed at 150 and 225°C, respectively) with total weight loss 12%. The further heating of the treated sample shows the appearance of two thermal effects on the DTA curve without weight loss: (1) Exothermal effect at 405°C which can be connected with crystallization process of $ZnMoO_4$ that can be partially in amorphous state which co-exists with crystalline phase of $ZnMoO_4$ fixed by XRD and (2) Endothermal effect with maximum at 720°C which is correspond to melting of nanodispersed of β-MoO_3. So, it was confirmed that ultrasonic activation of Zn/Mo oxide mixture allows the formation of $ZnMoO_4$ phase which can contain the part of the composition in partially amorphous state and formation of nanodimensions particles of MoO_3 with melting point lower at 70°C than the massive molybdena. It is necessary to note that the similar changes were fixed at mechanochemical treatment of oxide Zn/Mo system[35-37].

Due to the constant growth of world production of bioethanol, the production of intermediate chemical products by its transformation is considered as a promising way for the synthesis of other chemicals[43-47]. Results of the selective ethanol oxidation on the MoO_3 and some binary systems used

Table 4: Some properties of CeO_2/MoO_3 = 1:1 composition

					Catalytic properties at X = 100%	
Samples	*L α-MoO_3, 020/040 (nm)	S_{BET} (m^2 g^{-1})	V_Σ (cm^3 g^{-1})	S (%)	T_r (°C)	S_{ac} (%)
Initial	93/61	2	0.03	50	300	88
After UST	70/66	6	0.06	95	195	89

L: Average crystallite size, determined from the reflex of MoO_3, S_{BET}: Specific surface area (BET) of the sample, V_Σ: Total pore volume, S: Sorption degree (efficiency dye removal), T_r: Reaction temperature, S_{Ac}: Selectivity of acetaldehyde, X: Ethanol conversion

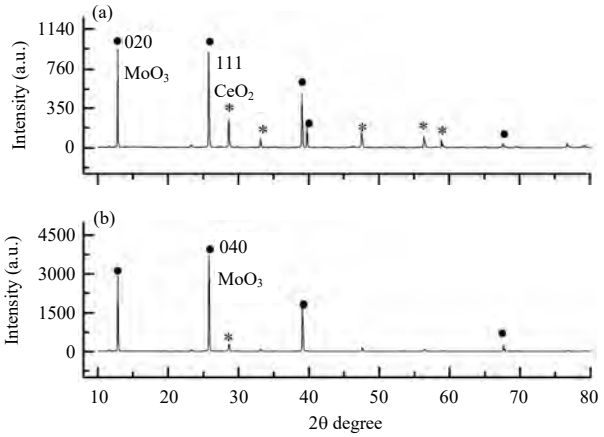

Fig. 4(a-b): Diffractograms of the CeO_2/MoO_3 = 1:1 composition, (a) Initial and (b) After UST

as catalysts were earlier reported[48-50]. The results of the study of catalytic activity of the initial and treated zinc-molybdenum oxides mixtures in selective ethanol oxidation are presented in Table 1. The catalytic tests were carried out in a flow type installation using the stainless steel micro-reactor in a temperature range of 25-300° C . The reaction mixture which contain 1% ethanol in air was used. The concentrations of initial reagents and reaction products were determined on-line on gas chromatographs with a flame-ionization and thermal conductivity detectors.

The comparison of the catalytic properties of initial and treated samples shows the enhancement in catalytic activity after UST. The increase of ethanol conversion and the reduction of the reaction temperature were observed (Table 1). This fact can be explained by a decrease of catalyst particle size and corresponding increase of specific surface area (Table 1) after treatment that leads, respectively, to an increase of the number of catalytic active centers available for reagent. It should be noted that the ethanol conversion in the case of treated sample equal to 100% can be achieve on 62°C lower (at 255°C) in comparison with initial sample.

The significant change of acetic aldehyde selectivity, namely its increasing for the sample after UST was also observed (Table 1). It can be connected with formation of nanosized zinc molybdate phase which is an active component of the catalyst in ethanol selective conversion to acetic aldehyde and provides the stability of its formation selectivity at suppression of parallel reaction of ethylene formation. It is necessary to note that the sample synthesized by UST method demonstrates a high stability of selectivity with ethanol conversion change as the acetaldehyde selectivity is equal to 100% at ethanol conversion 90% and reduced only insignificantly at conversion equal to 100%. In same time the $ZnMoO_4$ phase synthesized by the traditional method showed a decrease in selectivity already after 75% conversion of alcohol[51].

It should be noted that a decrease of full ethanol conversion temperature on treated sample at high values of selectivity and productivity (1.8 mol/kg/h) shows that process of ethanol oxidation on this catalyst can be consider as a promising alternative to the well-known industrial processes (Wacker process) of acetaldehyde production.

Sonochemical treatment of CeO_2/MoO_3 system: It is worth noting that similar studies are already done by Zazhigalov *et al.*[52] and Sobhani-Nasab *et al.*[53] connected with the study of Ce/Mo oxides mixtures properties and influence of ultrasonic treatment on oxide Ce/Mo mixtures transformation was studied[52]. So, in this section the results of influence UST on the physical and chemical properties of CeO_2/MoO_3 = 1:1 mixture will be presented.

The results of X-ray diffraction (Fig. 4a, b) demonstrated the presence in initial mixture of the reflexes of crystalline phases of α-MoO_3 orthorhombic modification and CeO_2 with cubic fluorite structure. It was found that sonochemical activation leads to increase of all MoO_3 reflexes intensity. On the other hand the change of dominant reflex of molybdenum oxide phase was observed which can be connected with anisotropic deformation of this phase in treatment process. It was found that after UST the decrease of reflex intensity and their broadening were observed that can be due to decrease of particle size of this oxide. The calculations of average particles size of CeO_2 demonstrate their decrease after UST while for MoO_3 somewhat different changes of crystals dimensions were observed (Table 4). The data presented in Table 4 showed that the treatment leads to a decrease of particles dimensions plane and their sizes plane rest practically without change.

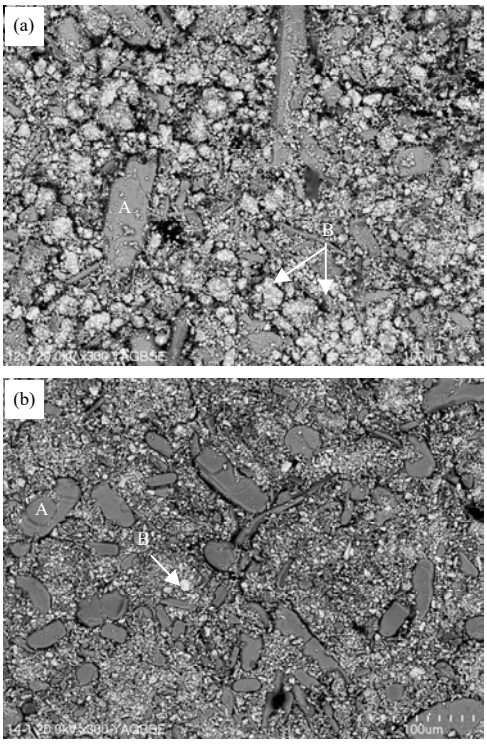

Fig. 5(a-b): SEM microphotographs of CeO_2/MoO_3 = 1:1 composition, (a) Initial and (b) After UST

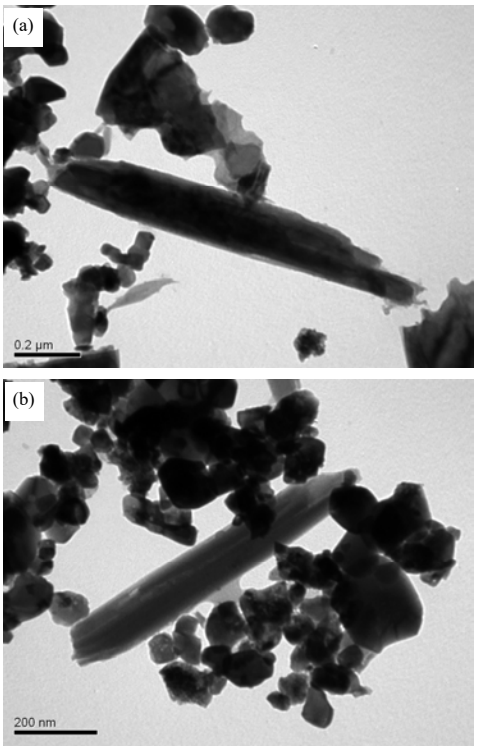

Fig. 6(a-b): TEM images of CeO_2/MoO_3 = 1:1 composition, (a) Initial and (b) After UST

Table 5: Analysis of the CeO_2/MoO_3 = 1:1 composition by EDS method

		Element content (%)	
Samples	Analysis site	Ce	Mo
Initial	A	3.47	96.53
	B	100.00	-
After UST	A	-	100.00
	B	95.97	4.03
	Full surface	48.94	51.06

So, the obtained results permit to conclude that sonochemical treatment of oxide Ce/Mo mixture leads to the chaotic destruction of CeO_2 and anisotropic deformation of MoO_3 without chemical reaction between components (unlike to the data presented by Leong *et al.*[5]) occurs.

The IR spectra of CeO_2/MoO_3 samples were recorded to confirm the changes of the structure after treatment. In spectrum of initial sample the bands at 933, 830, 804, 670, 626 and 416 cm^{-1} assigned to the Mo=O stretching mode, ν_s O-Mo-O symmetric stretching of the distorted octahedral (MoO_6) units, ν Mo-O vibrations, symmetric stretching vibrations in bridging ν_s Ce-O-Ce linkages, distorted octahedral (MoO_6) units as an asymmetric stretching ν_{as} O-Mo-O and ν_{as} Ce-O terminal bonds of stretching modes, respectively[54-57] were observed. It was found that UST leads to a change of sample spectrum. The band of Mo=O bond in molybdenum oxide shifts from 933-954 cm^{-1} that is due to increase of bond length and it is characteristic for layered orthorhombic MoO_3 phase. The peaks at 830, 804 (O-Mo-O bond) and 626 cm^{-1} (Mo-O-Mo bond) decrease their intensity. These changes well correspond to propose from XRD data anisotropic deformation of MoO_3 and formation of defects and the good agreement with SEM and TEM results is observed. The band at 670 cm^{-1} which is attributed to Ce-O-Ce bond shifts to 684 cm^{-1} which can testifies the chaotic destruction of this oxide as result of treatment with correspondence with XRD data.

The SEM images presented in Fig. 5a-b showed the general morphological aspect of the powder particles and decrease of oxides particles size after treatment. It is necessary to pay attention on the results of surface analysis which were obtained by EDS (Table 5). According to obtained results (Fig. 5a-b) both initial and modified samples are characterized by the presence of two types particles: big oblong particles (A) which according to EDS data (Table 5) can be destined to MoO_3 and most finely dispersed particles (B) which correspond to CeO_2. This fact was confirmed by TEM method also (Fig. 6a, b).

It was found that after sonochemical activation of the CeO_2/MoO_3 = 1:1 composition a decrease of the crystal size up to 25-100 nm (established by TEM method) occurs

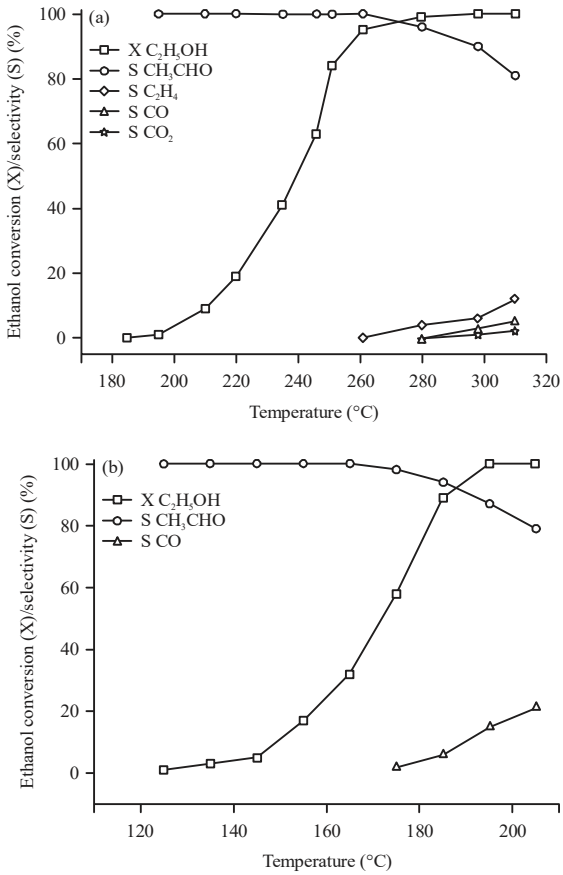

Fig. 7(a-b): Temperature dependence of ethanol conversion and selectivity of reaction product formation on, (a) Initial sample CeO_2/MoO_3 and (b) After UST

(Fig. 6a, b). The surface of the sample becomes smoother and oblong-like of MoO_3 crystals formed rounded nanoparticles as a result of treatment (Fig. 5b) that correspond to the data already presented[15-17], while for particles of CeO_2 the uniform distribution with less dimensions are characteristic. The observed particles size practically corresponds to the data obtained by XRD method (Table 4) and confirmed the chaotic destruction of CeO_2 particles from 50-150 up to 25-35 nm and anisotropic deformation of MoO_3. It should be noted that in the case of mechanochemical treatment of this system the core-shell structure particles (molybdenum oxide was supported on the ceria) were formed while UST leads to a decrease of oxides particles size of initial components milling only.

The ultrasound treatment influenced on porous structure of CeO_2/MoO_3 sample (Table 4), namely the enhancement of porous volume and specific surface area were observed that can play a role in adsorption and catalytic properties of studied samples.

The CeO_2/MoO_3 = 1:1 samples were tested as sorbents of Safranin T dye from water solution (C(safranin T) = 5.7×10^{-5}-2.3×10^{-4} mol L^{-1}), which can be used as marker of toxic substances of organic nature. The results of investigation show the enhancement of sorption capacity to safranin T for the sample after UST. In turn, the removal efficiency of the dye from the water solution by sonomodified sorbents is 95% while the initial sample showed only 50% of dye absorption. In this case, a specific surface area and volume of adsorption pores play a significant role. Also, it can be assumed that adsorption process on Ce/Mo oxides samples occurs by ion-exchange mechanism while the molecule of safranin T dye has π-bonds and it can to form the bond with sorbent surface.

The catalytic activity of CeO_2/MoO_3 = 1:1 samples in ethanol selective oxidation was measured and the obtained results presented in Table 4. The comparison of the results of sonomodified catalyst with initial sample (Fig. 7a, b) showed that full alcohol conversion on treated sample can be achieved at much lower temperature (Table 4, Fig. 7b) and selectivity to acetic aldehyde formation in this case is higher. Also as presented that UST permits to obtain the maximal values of selectivity and yield of acetic aldehyde (89%) at 195°C, while in initial sample at the same temperature the yield of the main product is only 4%.

According to Solsona *et al.*[58] and Zazhigalov *et al.*[36], the increase of catalytic activity of the samples at the same temperature (Fig. 7a, b) can be connected with an increase of specific surface area and decrease of particles size of the CeO_2/MoO_3 composition (Table 4, Fig. 7) as a result of UST. On the other hand, an increase of catalytic effectiveness can be connected with an appearance of structural defects as a result of milling in the treatment and more precise contacts between oxides. The obtained results showed (Fig. 8) that the yield of acetaldehyde (87-89%) remains without change after 15 h of operation. Reaction temperature is 195°C.

So, the study of ultrasonic treatment of mixed oxide Ce/Mo system influence on its catalytic properties showed the increase of catalytic activity in acetic aldehyde formation process from ethanol due to the presence of nanosized oxides particles with the possibility of hard contact between them and nanoparticles of cerium oxide can plays role of promoter or oxygen dopant.

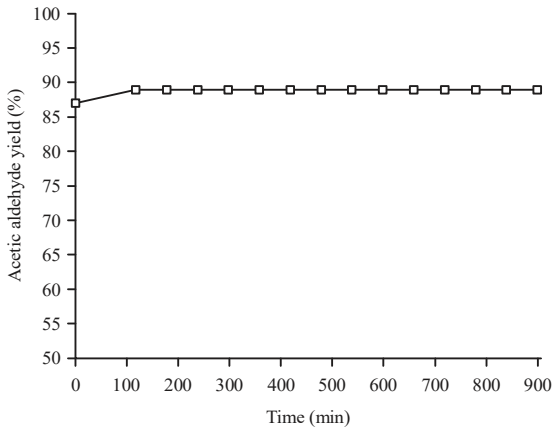

Fig. 8: Effect of time operation on acetaldehyde yield on sonomodified CeO_2/MoO_3 = 1:1 catalyst

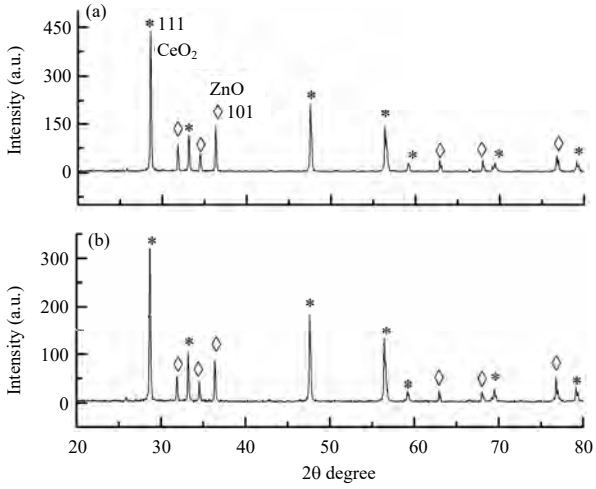

Fig. 9(a-b): Diffractograms of the ZnO/CeO_2 = 1:1 composition, (a) Initial and (b) After UST

Table 6: Some properties of ZnO/CeO_2 = 1:1 samples

	*L (nm)						
Samples	CeO_2	ZnO	S_{BET} ($m^2 g^{-1}$)	V_Σ ($cm^3 g^{-1}$)	λ (nm)	E_g (eV)	$K_d \times 10^4$ (sec^{-1})
Initial	60	57	2	0.01	396	3.13	0.2
After UST	29	30	4	0.05	392	3.16	3.3

*L: Average crystallite size, determined from the maximum intensive reflex, S_{BET}: Specific surface area (BET) of the sample, V_Σ: Total pore volume, λ: Absorption edge, E_g: Band-gap energy, K_d: Constant of the rate degradation of safranin T in water solution

Ultrasonic modification of ZnO/CeO_2 system: The logical step after the study of ZnO/MoO_3 and CeO_2/MoO_3 mixtures sonochemical treatment were the investigation of UST influence on the physico-chemical properties of ZnO/CeO_2 system. The results obtained at ZnO/CeO_2 = 1:1 mixture treatment and properties of prepared sample is presented in Fig. 9a-b.

It was found that ultrasonic treatment leads to insignificant changes in general view of diffractogram of initial sample namely a decrease of intensity basic reflexes of oxides without the change of dominant reflex that can be connected with isotropic deformation of ZnO and CeO_2 and indicates the particles size reduction of initial oxides.

The calculations of oxides particles size demonstrate their decrease in two times after treatment in comparison with initial mixture (Table 6). These results are in good agreement with adsorption data. An increase of specific surface area of the sample after treatment is the result of reduction in the size of the oxides particles, but the adsorption data showed that in the same time an increase in total pore volume carries out.

The study of the oxide mixtures Zn/Ce = 1:1 by thermogravimetric method shown that thermal treatment of the sample after UST accompanied by one-stage dehydration with a corresponding endothermic effect at 163°C. There is a difference between the initial sample and after its sonochemical activation. In the case of initial sample the water removal proceeds in two stages in the temperature range 150-230°C. Such changes can be related with the formation of homogeneous porous structure of the sample as a result of treatment. For treated sample on the DTA curve, there are two exothermic effects with maximums at 460 and 660°C (absent in DTA initial sample), which can correspond to the crystallization process of ZnO and polymorphic transformation of the composite, respectively, without mass loss. So, it can be supposed that UST of oxide mixture leads to not only particles size decrease, but to their partial amorphization also.

The results of the IR-spectroscopy study of ZnO/CeO_2 = 1:1 samples showed that ultrasonic treatment leads to a decrease of the intensity of absorption bands of adsorbed water molecules stretching and deformation vibrations at 3200 and 1692 cm^{-1}, respectively, that caused by a decrease in the content of surface groups OH^- due to modification of the sample.

The spectrum of initial sample showed the presence of the main absorption bands at 613 and 1195 cm^{-1}, which belong to the Zn-O and linear Ce-O-Ce bonds, respectively. It was found that ultrasonic modification of the sample leads to a slight shift of these absorption bands in the shortwave region up to 609 and 1177 cm^{-1}, correspondingly and it is accompanied by the appearance of vibrations of the lattice Ce-O bond at 970 cm^{-1} that caused by the bond redistribution Ce-O as a result of treatment.

The electronic spectrum of the sonoactivated Zn/Ce = 1:1 oxide mixture is slightly different from its initial sample, although there the some shift in UV region occurs (Table 6). It was found that the calculated value of the band gap of activated composite material are somewhat smaller

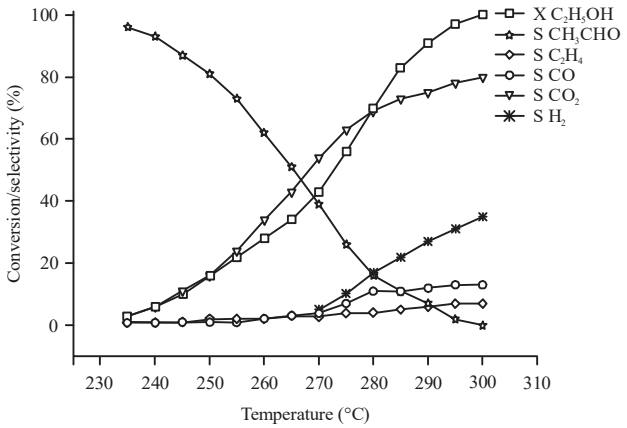

Fig. 10: Temperature dependence of ethanol conversion (X) and selectivity to products formation (S) on the sonomodified ZnO/CeO_2 = 1:1 catalyst

in comparison with the values of the band gap of both mechanically activated samples (60) and pure zinc oxide (E_g (ZnO) = 3.24 eV), but close to value Eg, characteristic for cerium oxide (Eg (CeO_2) = 3.19 eV). Insignificant increase in band gap of the sample after activation is likely due to a decrease in the size of crystals, electron transitions and the implementation of direct interband transitions with energy exceeding Eg.

Thus, in the absorption spectrum of ZnO/CeO_2 = 1:1 treated composition, the so-called "blue" shifting is observed in comparison with the absorption band of the initial sample, which may be caused by the effect of dispersion changing of the system due to its processing. These data showed the prospect of these samples study as photocatalysts.

The photocatalytic activity of ZnO/CeO_2 = 1:1 samples was studied in the reaction of Safranin T dye degradation (C(safranin T = 1.3×10^{-5} mol L^{-1})) in water solution at visible irradiation. It was found that modified sample is more active in comparison with initial sample. The dye photodegradation is described by the kinetic equation of the first order. This fact can be explained by displacement of the absorption edge into the shortwave region as well as by increasing the value of the specific surface area which is available for dye molecules due to the dispersion of ZnO/CeO_2 composition in the treatment process. It should be noted that the destruction rate of the dye in solution on sonoactivated sample is slightly higher than in the case of samples after mechanochemical treatment[59,60].

The initial ZnO/CeO_2 = 1:1 mixture demonstrated low catalytic activity in ethanol oxidation up to 300°C (ethanol conversion at this temperature is equal to 56%). The sample after UST is more active in this process (Fig. 10).

The ethanol conversion at 300°C reaches 100%, but acetaldehyde selectivity fast decreased and practically equal to zero at this temperature. The dominant process is full ethanol oxidation that can be connected with the CeO_2 properties as oxygen dopant[61], but interesting fact is an increase of hydrogen formation selectivity with the increase of the reaction temperature. So, the other mechanism of ethanol oxidation has place at absence of molydbena in catalyst composition.

CONCLUSION

It was found that ultrasonic treatment of mixture ZnO/MoO_3 system leads to formation of nanodispersed phase of triclinic modification α-$ZnMoO_4$ in the needle form. In the case of Ce/Mo, system the decrease of initial components without reaction between oxides carries out. The sonoactivation of ZnO/CeO_2 system leads to increase of photocatalytic activity in safranin T dye degradation which makes them promising photocatalysts of environmental protection processes.

It was shown that UST of MoO_3-containing systems (ZnO/MoO_3 and CeO_2/MoO_3) allows to decrease of temperature reaction in ethanol oxidation and make it possible to obtain acetic aldehyde with maximal yield 94% at low temperature (about 200°C). In general the high selectivity to acetaldehyde and productivity for this product with the stability of the catalysts operation show that ethanol oxidation on the sonomodified catalysts can be considered as an alternative to well-known Wacker process.

SIGNIFICANCE STATEMENT

The significance of current research is due to the use of a new and "environment friendly" method of nanocomposite materials synthesis in which the oxides of Zn, Ce and Mo are used as initial materials. The perspective of the use of the sonomodified zinc-cerium system in photocatalytic purification of water from organic dyes is shown. For the first time, it was found that sonomodified oxide Mo-containing Zn and Ce systems exhibit high catalytic activity in the ethanol selective oxidation reaction to acetic aldehyde at 200°C with a maximum yield of 96-97% and a productivity of about 2 mol $kg^{-1}_{cat}\times h$, which can compete with the well-known Wacker process for the production of acetaldehyde.

The reliability and validity of the results and conclusions are ensured by the parallel use of various physicochemical methods of studying the structure of the surface of the synthesized materials and sorption processes and checking the reproducibility of all obtained results. An additional factor in verifying the results obtained was their comparison with previous studies. Thus, a theory on sonochemical method by which nanocomposites are formed is presented.

ACKNOWLEDGMENTS

This work was financially supported by NASU Programs: grant number 13/19. The authors are grateful to research assistant O.A. Diyuk (ISPE NAS of Ukraine) for assistance in catalytic testing of samples.

Authors also thankful to the Research Journal of Nanoscience and Nanotechnology for publishing this article free of cost and to Karim Foundation for bearing the cost of article production, hosting as well as liaison with abstracting and indexing services and customer services.

REFERENCES

1. Chatel, G., 2018. How sonochemistry contributes to green chemistry? Ultrasonics Sonochem., 40,: 117-122.
2. Bang, J.H. and K.S. Suslick, 2010. Applications of ultrasound to the synthesis of nanostructured materials. Adv. Mater., 22: 1039-1059.
3. Mason, T.J. and T.P. Lorimer, 2003. Applied Sonochemistry: The Uses of Power Ultrasound in Chemistry and Processing. Wiley-VCH, Weinheim, ISBN: 978-3-527-60054-0, Pages: 293.
4. Shevchuk, L. and V. Starchevskyy, 2014. Cavitation. Physical, Chemical, Biological and Technological Aspects. Lviv Polytechnic Publishing House, Lviv, Pages: 376, (In Ukrainian).
5. Leong, T., M. Ashokkumar and S. Kentish, 2011. The fundamentals of power ultrasound-A review. Acoustics Aust., 39: 43-63.
6. Margulis, M., 1984. Bases of Sonochemistry. Higher School Publishing House, Moscow, Pageds: 272, (In Russian).
7. Linares, P., F. Lazaro, M.D.L. de Castro and M. Valcarcel, 1988. Analytical sonochemistry: A review. J. Anal. Methods Chem., 10: 88-94.
8. Pirsol, I., 1975. Cavitation. Mir, Moscow, Pages: 95, (In Russian).
9. Kumar, R.V., Y. Koltypin, X.N. Xu, Y. Yeshurun, A. Gedanken and I. Felner, 2001. Fabrication of magnetite nanorods by ultrasound irradiation. J. Applied Phys., 89: 6324-6328.
10. Jeevanandam, P., Y. Koltypin and A. Gedanken, 2001. Synthesis of nanosized α-nickel hydroxide by a sonochemical method. Nano Lett., 1: 263-266.
11. Avivi, S., Y. Mastai, G. Hodes and A. Gedanken, 1999. Sonochemical hydrolysis of Ga^{3+} ions: Synthesis of scroll-like cylindrical nanoparticles of gallium oxide hydroxide. J. Am. Chem. Soc., 121: 4196-4199.
12. Avivi, S., Y. Mastai and A. Gedanken, 2000. Sonohydrolysis of In^{3+} ions: Formation of needlelike particles of indium hydroxide. Chem. Mater., 12: 1229-1233.
13. Shafi, K.V.P.M., I. Felner, Y. Mastai and A. Gedanken, 1999. Olympic ring formation from newly prepared barium hexaferrite nanoparticle suspension. J. Phys. Chem. B, 103: 3358-3360.
14. Mao, C.J., H.C. Pan, X.C. Wu, J.J. Zhu and H.Y. Chen, 2006. Sonochemical route for self-assembled V_2O_5 bundles with spindle-like morphology and their novel application in serum albumin sensing. J. Phys. Chem. B, 110: 14709-14713.
15. Jeevanandam, P., Y. Diamant, M. Motiei and A. Gedanken, 2001. The effect of ultrasound irradiation on polycrystalline MoO_3. Phys. Chem. Chem. Phys., 3: 4107-4112.
16. Chen, J.J., H.B. Yang, L.X. Chang, W.Y. Fu, Y. Zeng, H.Y. Zhu and G.T. Zou, 2007. Sonochemical preparation and characterization of photochromic MoO_3 nanoparticles. Front. Phys. China, 2: 92-95.
17. Bin, L., Y. Daheng, C. Jiuju, Y. Xiaolei and M. Qinggang, 2011. Sonochemical preparation and characterization of MoO_3 and MoS_2 nanoparticles. Proceedings of the International Conference on Management Science and Industrial Engineering (MSIE), January 8-11, 2011, Harbin, China, pp: 1083-1086.
18. Krishnan, C.V., J. Chen, C. Burger and B. Chu, 2006. Polymer-assisted growth of molybdenum oxide whiskers via a sonochemical process. J. Phys. Chem. B, 110: 20182-20188.
19. Manivel, A., G.J. Lee, C.Y. Chen, J.H. Chen, S.H. Ma, T.L. Horng and J.J. Wu, 2015. Synthesis of MoO_3 nanoparticles for azo dye degradation by catalytic ozonation. Mater. Res. Bull., 62: 184-191.
20. Pholnak, C., C. Sirisathitkul, S. Suwanboon and D.J. Harding, 2014. Effects of precursor concentration and reaction time on sonochemically synthesized ZnO nanoparticles. Mater. Res., 17: 405-411.
21. Costa, B.C., C. Morilla-Santos and P.N. Lisboa-Filho, 2015. Effects of time exposure and low power sonochemical treatment on ZnO mesostructures. Mater. Sci. Semicond. Process., 35: 81-89.
22. Arruda, L.B., M.O. Orlandi and P.N. Lisboa-Filho, 2013. Morphological modifications and surface amorphization in ZnO sonochemically treated nanoparticles. Ultrason. Sonochem., 20: 799-804.
23. Kandjani, A.E., M.F. Tabriz and B. Pourabbas, 2008. Sonochemical synthesis of ZnO nanoparticles: The effect of temperature and sonication power. Mater. Res. Bull., 43: 645-654.
24. Tabatabee, M., R. Shaikhalishahi and R. Mohammadinasab, 2015. Sonochemical preparation and characterization of CeO_2 nanoparticles using polyethylene glycols as a neutral surfactant. Res. Chem. Intermed., 41:113-116.
25. Zhang, D., H. Fu, L. Shi, C. Pan, Q. Li, Y. Chu and W. Yu, 2007. Synthesis of CeO_2 nanorods via ultrasonication assisted by polyethylene glycol. Inorg. Chem., 46: 2446-2451.
26. Wang, H., J.J. Zhu, J.M. Zhu, X.H. Liao, S. Xu, T. Ding and H.Y. Chen, 2002. Preparation of nanocrystalline ceria particles by sonochemical and microwave assisted heating methods. Phys. Chem. Chem. Phys., 4: 3794-3799.

27. Alammar, T., H. Noei, Y. Wang, W. Grünert and A.V. Mudring, 2015. Ionic liquid-assisted sonochemical preparation of CeO_2 nanoparticles for CO oxidation. ACS Sustainable Chem. Eng., 3: 42-54.
28. Sachuk, O., N. Kopachevska, L. Kuznetsova, V. Zazhigalov and V. Starchevskyy, 2017. Influence of ultrasonic treatment on the properties of ZnO-MoO_3 oxide system. Chem. Chem. Technol., 11:152-157.
29. Zazhigalov, V.A., O.V. Sachuk, N.S. Kopachevska, V.L. Starchevskyy and Z. Sawlowicz, 2017. Effect of ultrasonic treatment on formation of nanodimensional structures in ZnO-MoO_3 system. Theor. Exp. Chem., 53: 53-59.
30. Keereeta, Y., T. Thongtem and S. Thongtem, 2014. Effect of medium solvent ratios on morphologies and optical properties of α-$ZnMoO_4$, β-$ZnMoO_4$ and $ZnMoO_4$• $0.8H_2O$ crystals synthesized by microwave-hydrothermal/ solvothermal method. Superlattices Microstruct., 69: 253-264.
31. Ait ahsaine, H., M. Zbair, M. Ezahri, A. Benlhachemi and M. Arab *et al*., 2015. Rietveld refinements, impedance spectroscopy and phase transition of the polycrystalline $ZnMoO_4$ ceramics. Ceramics Int., 41:15193-15201.
32. Agarwal, D.C., D.K. Avasthi, S. Varma, F. Kremer, M.C. Ridgway and D. Kabiraj, 2014. Phase transformation of $ZnMoO_4$ by localized thermal spike. J. Applied Phys., Vol. 115, No. 16. 10.1063/1.4872259
33. Karekar, S.E., B.A. Bhanvase, S.H. Sonawane, M.P. Deosarkar, D.V. Pinjari and A.B. Pandit, 2015. Synthesis of zinc molybdate and zinc phosphomolybdate nanopigments by an ultrasound assisted route: Advantage over conventional method. Chem. Eng. Process.: Process Intensif., 87: 51-59.
34. Zhang, G., S. Yu, Y. Yang, W. Jiang, S. Zhang and B. Huang, 2010. Synthesis, morphology and phase transition of the zinc molybdates $ZnMoO_4$• $0.8H_2O$/α-$ZnMoO_4$/$ZnMoO_4$ by hydrothermal method. J. Crystal Growth, 312: 1866-1874.
35. Sachuk, O.V., V.O. Zazhigalov, L.S. Kuznetsova and M.M. Tsyba, 2016. Properties of Zn-Mo oxide system synthesized by mechanochemical treatment. Chem. Phys. Technol. Surf., 7: 309-321.
36. Zazhigalov, V.A., K. Wieczorec-Ciurowa, E.V. Sachuk, E.A. Diyuk and I.V. Bacherikova, 2018. Mechanochemical synthesis of nanodispersed molybdenum oxide catalysts. Theor. Exp. Chem., 54: 225-234.
37. Zazhigalov, V.A., E.V. Sachuk, N.S. Kopachevskaya, I.V. Bacherikova, K. Wieczorec-Ciurowa and S.N. Shcherbakov, 2016. Mechanochemical synthesis of nanodispersed compounds in the ZnO-MoO_3 system. Theor. Exp. Chem., 52: 97-103.
38. Chiang, T.H. and H.C. Yeh, 2013. The synthesis of α-MoO_3 by ethylene glycol. Materials, 6: 4609-4625.
39. Irmawati, R. and M. Shafizah, 2009. The production of high purity hexagonal MoO_3 through the acid washing of as-prepared solids. Int. J. Basic Applied Sci., 9: 34-36.
40. Cavalcante, L.S., E. Moraes, M.A.P. Almeida, C.J. Dalmaschio and N.C. Batista *et al*., 2013. A combined theoretical and experimental study of electronic structure and optical properties of β-$ZnMoO_4$ microcrystals. Polyhedron, 54: 13-25.
41. Talam, S., S.R. Karumuri and N. Gunnam, 2012. Synthesis, characterization and spectroscopic properties of ZnO nanoparticles. ISRN Nanotechnol.,. 10.5402/2012/372505.
42. Mancheva, M., R. Iordanova, A.A. Kamenova, A. Stoyanova, Y. Dimitriev and B. Kunev, 2007. Influence of mechanical treatment on morphology of the MoO_3 nanocrystals. Nanosci. Nanotechnol., 7: 74-76.
43. Rana, P.H. and P.A. Parikh, 2017. Bioethanol valorization via its gas phase oxidation over Au &/or Ag supported on various oxides. J. Ind. Eng. Chem., 47: 228-235.
44. Yoshitake, H., Y. Aoki and S. Hemmi, 2006. *Mesoporous titania* supported-molybdenum catalysts: The formation of a new mesophase and use in ethanol-oxygen catalytic reactions. Microporous Mesoporous Mater., 93: 294-303.
45. Yang, J.I., D.W. Lee, J.H. Lee, J.C. Hyun and K.Y. Lee, 2000. Selective and high catalytic activity of $Cs_nH_{4-n}PMo_{11}VO_{40}$ ($n \geq 3$) for oxidation of ethanol. Applied Catal. A: Gen., 194: 123-127.
46. Gonçalves, F.M., P.R. Medeiros and L.G. Appel, 2001. The role of cerium in the oxidation of ethanol over SnO_2-supported molybdenum oxides. Applied Catal. A: Gen., 208: 265-270.
47. Eckert, M., G. Fleischmann, R. Jira, H. Bolt and K. Golka, 2006. Acetaldehyde. In: Ullmann's Encyclopedia of Industrial Chemistry, Wiley-VCH (Eds.)., Wiley VCH Verlag GmbH & Co. KGaA., Weinheim.
48. Kopachevska, N., S. Khalameida and V. Zazhigalov, 2015. Mechanochemical activation of molybdenum containing catalysts. CP., 24: 1-12.
49. Sidorchuk, V.V., S.V. Khalameida, N.S. Litvin and V.A. Zazhigalov, 2010. Vanadium- and molybdenum-containing compositions prepared by mechanochemical and following thermal treatments of V_2O_5/$(NH_4)_2Mo_2O_7$ (V/Mo = 0.7/0.3). Russian J. Inorg. Chem., 55: 848-856.
50. Litvin, S.N., 2011. Mechanochemistry of complex oxide systems based on molybdenum and vanadium. Ph.D. Thesis, Institute for Sorption and Problems of Endoecology of NAS of Ukraine, Kyiv.
51. Sachuk, O.V., 2019. Nanodispersed Zn-MoO_3 catalysts of selective ethanol oxidation synthesized by nontraditional methods. Dopov. Nac. Akad. Nauk Ukr., 6: 48-53, (In Ukrainian).
52. Zazhigalov, V.A., O.V. Sachuk, O.A. Diyuk, V.L. Starchevskyy and S.V. Kolotilov *et al*., 2018. The Ultrasonic Treatment as a Promising Method of Nanosized Oxide CeO_2-MoO_3 Composites Preparation. In: Nanochemistry, Biotechnology, Nanomaterials and Their Applications, NANO 2017. Proceedings in Physics, Vol. 214, Fesenko, O. and L. Yatsenko (Eds.)., Springer, Cham, pp: 297-309.

53. Sobhani-Nasab, A., M. Maddahfar and S.M. Hosseinpour-Mashkani, 2016. $Ce(MoO_4)_2$ nanostructures: Synthesis, characterization and its photocatalyst application through the ultrasonic method. J. Mol. Liq., 216: 1-5.
54. Sohn, J.R., E.W. Chun and T.I. Pae, 2003. Spectroscopic studies on ZrO_2 modified with MoO_3 and activity for acid catalysis. Bull. Korean Chem. Soc., 24: 1785-1792.
55. Seguin, L., M. Figlarz, R. Cavagnat and J.C. Lassègues, 1995. Infrared and Raman spectra of MoO_3 molybdenum trioxides and $MoO_3 \cdot xH_2O$ molybdenum trioxide hydrates. Spectrochim. Acta Part A: Mol. Biomol. Spectrosc., 51:1323-1344.
56. Epifani, M., P. Imperatori, L. Mirenghi, M. Schioppa and P. Siciliano, 2004. Synthesis and characterization of MoO_3 thin films and powders from a molybdenum chloromethoxide. Chem. Mater., 16: 5495-5501.
57. Rathod, S.B., M.K. Lande, B.R. Arbad and A.B. Gambhire, 2014. Preparation, characterization and catalytic activity of $MoO_3/CeO_2–ZrO_2$ solid heterogeneous catalyst for the synthesis of β-enaminones. Arabian J. Chem., 7: 253-260.
58. Solsona, B., V.A. Zazhigalov, J.L. Nieto, I.V. Bacherikova and E.A. Diyuk, 2003. Oxidative dehydrogenation of ethane on promoted VPO catalysts. Applied Catal. A: Gen., 249: 81-92.
59. Sachuk, O., V. Zazhigalov, L. Kuznetsova and S. Shcherbakov, 2017. The influence of mechanochemical activation on the Zn-Ce-O composition properties. Adsorption Sci. Technol., 35: 845-852.
60. Sachuk, O.V., V.A. Zazhigalov, O.P. Fedorovska, L.S. Kuznetsova and S.M. Shcherbakov, 2016. Mechanochemical activation influence of the ZnO/CeO_2 compositions on their structural characteristics and photocatalytic activity in safranin T degradation process. Catal. Petrochem., 25: 36-40.
61. Trovarelli, A., 1996. Catalytic properties of ceria and CeO_2-containing materials. Catal. Rev., 38: 439-520.